Thermal Aging Effects on Residual Stress and Residual Strain Distribution on Heat Affected Zone of Alloy 600 in Dissimilar Metal Weld

Junhyuk Ham[a], Kyoung Joon Choi[a] and Ji Hyun Kim[a*]
[a] *School of Mechanical and Nuclear Engineering, Ulsan National Institute of Science and Technology (UNIST), Ulju-gun, Ulsan 44919, Republic of Korea*
[*] *Corresponding author: kimjh@unist.ac.kr*

1. Introduction

Dissimilar metal weld (DMW), consisting of Alloy 600, Alloy 182, and A508 Gr.3, has been widely used as a joining material of the reactor pressure vessel penetration nozzle and the steam generator tubing for pressurized water reactors (PWR) because of its good mechanical strength, thermal conductivity, and corrosion resistance [1].

Primary water stress corrosion cracking (PWSCC) of vessel head penetrations fabricated from DMW was first observed in the early 1990s. Since then PWSCC has become a generic problem for DMW components in PWR plants [2].

Residual tensile stress is mainly nominated as a cause of SCC in light water reactors by IAEA report. So, to relax the residual stress, post-weld heat treatment is required after manufacturing process such as welding. However, thermal treatment has a great effect on the microstructure and the chromium depletion profile on Alloy 600, so called sensitization [1]. Therefore, Alloy 600 does not conduct post-weld heat treatment commonly and this causes high residual stress on the heat affected zone (HAZ).

By this reason, HAZ on Alloy 600 is critical to crack. According to G.A. Young et al., Crack growth rates (CGR) in the Alloy 600 HAZ were about 30 times faster than those in the Alloy 600 base metal tested under the same conditions. And according to Z.P. Lu et al., CGR in the Alloy 600 HAZ can be more than 20 times higher than that in its base metal [3].

There are some methods to measure the exact value of residual stress on the material surface. The most common way is X-ray diffraction method (XRD). The principle of XRD is based on lattice strains and depends on the changes in the spacing of the atomic planes in material. And there is a computer simulation method to estimate residual stress distribution which is called ANSYS.

The scanning acoustic microscope (SAM) which is based on the ultrasonic technique can also measure the residual stress. Comparing SAM with XRD, it has an advantage to surface treatment. Unlike XRD, SAM is not critically affected by surface preparation. This advantage can shorten preparing procedure of experiment and can increase the accuracy of the result since it is free from surface condition. Besides, according to preceding researches, SAM results match well with that of XRD and ANSYS on the same position of same material [4, 5]

According to L. Wang et al. compressive residual stress increases hardness and tensile residual stress decreases hardness of the material. And the effect of tensile stress is far more significant [6].

Thus, the main goal of this experiment is to investigate how the long-term thermal aging affects the residual stress of Alloy 600 HAZ by using Vickers hardness tester and SAM, and how residual stress distribution change affects the residual strain by using a function named kernel average misorientation (KAM) in electron backscattering diffraction (EBSD).

2. Experimental

2.1 Materials and specimens

By joining Alloy 600 and A508 Gr. 3 with Alloy 182 serving as dissimilar filler metal, representative mockup sample was fabricated with welding process which was qualified by the American Society of Mechanical Engineers (ASME) [7]. The chemical compositions of each metal is shown in Table 1.

$$\frac{t_{aging}}{t_{ref}} = exp\left[-\frac{Q\left(\frac{1}{T_{ref}} - \frac{1}{T_{aging}}\right)}{R}\right]$$

t_{aging} = Aging time [hr]
t_{ref} = Simulated operation time [hr]
T_{aging} = Aging temperature [K]
T_{ref} = Simulated operation temperature (320 °C) [K]
R = Gas constant [kJ/mol]
Q = Activation energy for Cr diffusion (about 180 kJ/mol)

Figure. 1. Diffusion equation to calculate the relation between temperature and time of reference case and aging case.

The heat treatment condition for thermal aging simulation was determined based on diffusion equation with activation energy of chromium through grain boundary. Since chromium is known to do important role to material properties. And also chromium precipitate affects the property of material a lot [8].

Heat treatment simulates the aged DMW which is used during 15 years and 30 years in the commercial nuclear power plant (operating at temperature about 320 °C). Both aging temperature and aging time are calculated under the diffusion equation in Figure 1.

Table. 1. Chemical composition (in wt.%) of dissimilar metal used in this experiment

Material	Composition									
	C	Si	Mn	P	S	Fe	Cu	Ni	Cr	etc.
Alloy 600	0.06	0.30	0.07	-	0.001	8.13	0.01	74.9	15.6	-
Alloy 182	0.05	0.37	7.42	0.01	0.01	4.48	0.01	70.9	14.9	1.77Nb+Ta 0.03Ti
A508 Gr.3	0.19	0.22	1.33	0.008	0.002	Bal.	0.02	0.91	0.19	0.47Mo, 0.02Al 0.003V

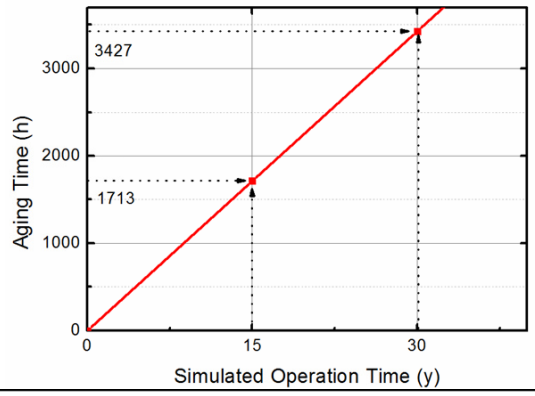

Specimen I.D.	t_{ref}	t_{aging}, T_{aging}
As-welded	-	-
HT400_Y15	15-yr	1713-hr at 400 ℃
HT400_Y30	30-yr	3427-hr at 400 ℃

Figure. 2. Aging time at the temperature 400 ℃ to simulate 15 years and 30 years at the temperature 320 ℃ in nuclear power plant respectively.

The heat treatment process is described in Figure 2. Heat treatment temperature was selected as 400 ºC. It can be said that higher temperature may reduce the simulating time, however, when the temperature goes above 450 ºC, some un-wanted phase can occur. Therefore, 400 ºC was chosen in this experiment.

According to the abovementioned values for the diffusion equation, the finally calculated aging time for 15 years at 320 ℃ is 1713 hours at 400 ℃ and the aging time for 30 years at 320 ℃ is 3427 hours at 400 ℃.

2.2 Experimental procedure

The specimens cut from the as-welded mockup sample were polished with emery paper of 320 grits, 600 grits, and 800 grits, diamond paste of 6 μm, 3 μm, and 1 μm. And finally vibration polishing was conducted with 0.05 μm colloidal silica/alumina solution during 48 hours to minimize mechanical deformation on the surface.

After the polishing process, the specimens were washed with acetone in 2 minutes, ethanol in 2 minutes, and distilled water in 20 seconds.

The hardness of each specimen was measured by Vickers hardness tester using a load of HV 0.01 (i.e. 0.01 kgf). Hardness measurements were conducted from Alloy 182 to Alloy 600.

The residual strain of each specimen at the Alloy 600 HAZ was observed by KAM mapping, a function of EBSD with step size 2μm.

3. Results and Discussions

3.1 Hardness

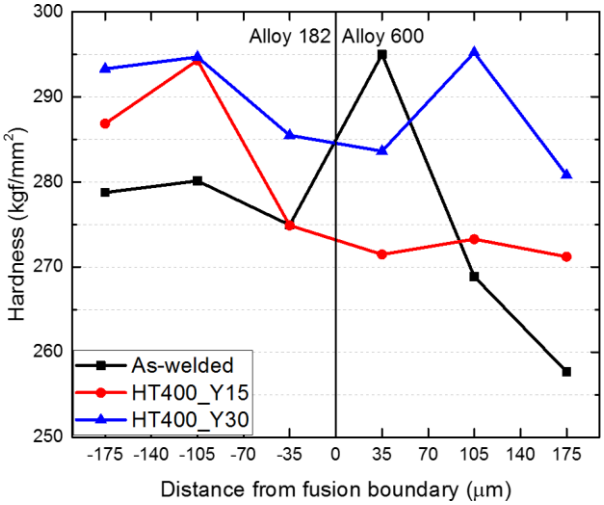

Figure. 3. Averaged Vickers hardness result near the fusion boundary between Alloy 182 and Alloy 600.

Figure 3 shows the averaged distribution of Vickers hardness which was measured near the fusion boundary between Alloy 182 and Alloy 600 of each case As-welded, HT400_Y15, and HT400_Y30. As the graph shows, there is an obvious tendency between the simulated aging time and Vickers hardness.

At the Alloy 600 HAZ of As-welded the hardness is much bigger than surroundings. This can be caused by near zone of compressive residual stress which was formed by welding process.

The tendency of hardness of HT400_Y15 specimen may be caused by relaxation of residual stress mechanism which is spreading out the stress to around. Therefore, the influence of both tensile and compressive residual stress became weaker than before and that makes each hardness increase or decrease.

The case of HT400_Y30, residual stress is almost relaxed. So the value of hardness recovered high as the graph shows.

3.2 Residual stress

It is well known that normalized velocity of leaky surface acoustic wave (ΔV_{saw}) is proportional to residual stress linearly [4, 5]. According to the result, there was a compact zone where the ΔV_{saw} value is negative at Alloy 600 HAZ near the fusion boundary. This directly means that compressive residual stress zone was formed on that region. When the tested point moved far from that point in both direction, ΔV_{saw} became positive. Therefore, it can be said that broad tensile residual stress zone was formed on the specimen but compressive zone at compact area near the fusion boundary was also formed.

This tendency was changed when the specimen had thermally treated about 15-yr. Through the whole tested points, ΔV_{saw} was positive but the magnitude became smaller than before. The narrow compressive zone which was found from As-welded specimen was gone. When the specimen underwent thermal treatment about 15-yr, tensile residual stress is spread through the entire area.

After aging 30-yr, the ΔV_{saw} decreased averagely compared with 15-yr case. This can be interpreted as remained tensile residual stress is almost relaxed.

This SAM result fits well with the result of Vickers hardness test result. Although it is impossible to measure the exact value of residual stress by using hardness test, the tendency of residual stress can be observed by using that method.

3.3 Kernel average misorientation

Figure 4 (a), As-welded case, KAM values are concentrated at certain regions. There are red dotted regions but no yellow ones. Figure 4 (b), HT400_Y15 case, yellow dotted regions are formed broadly compared with As-welded specimen. And finally Figure 4 (c), HT400_Y30 case, it is hard to find red and yellow dotted regions. There are just blue and green dotted regions only. This tendency can explain how the residual strain disappears. Residual strain spread to the surrounding.

As Figure 5 shows, low KAM decreases about 11%p from As-welded to HT400_Y15, and it increases about 23%p from HT400_Y15 to HT400_Y30. High KAM increases about 3%p from As-welded to HT400_Y15, and decreases about 13%p from HT400_Y15 to HT400_Y30. However, the fraction of very high KAM of HT400_Y15 was about 11%. So it should not be neglected.

The total value of KAM multiplying by fraction increased about 0.2 from As-welded to HT400_Y15, and decreased about 0.38 from HT400_Y15 to HT400_Y30.

According to Z. Lu et al. KAM value at the Alloy 600 HAZ is higher comparing with that of Alloy 600 base metal [9]. Furthermore, C. Ma et al. observed that a peak of KAM value at all grain boundaries is approximately 3 times higher than that of inside of the grain [10]. Summarizing these researches, the grain boundaries at Alloy 600 HAZ is the most vulnerable to the effect of residual strain.

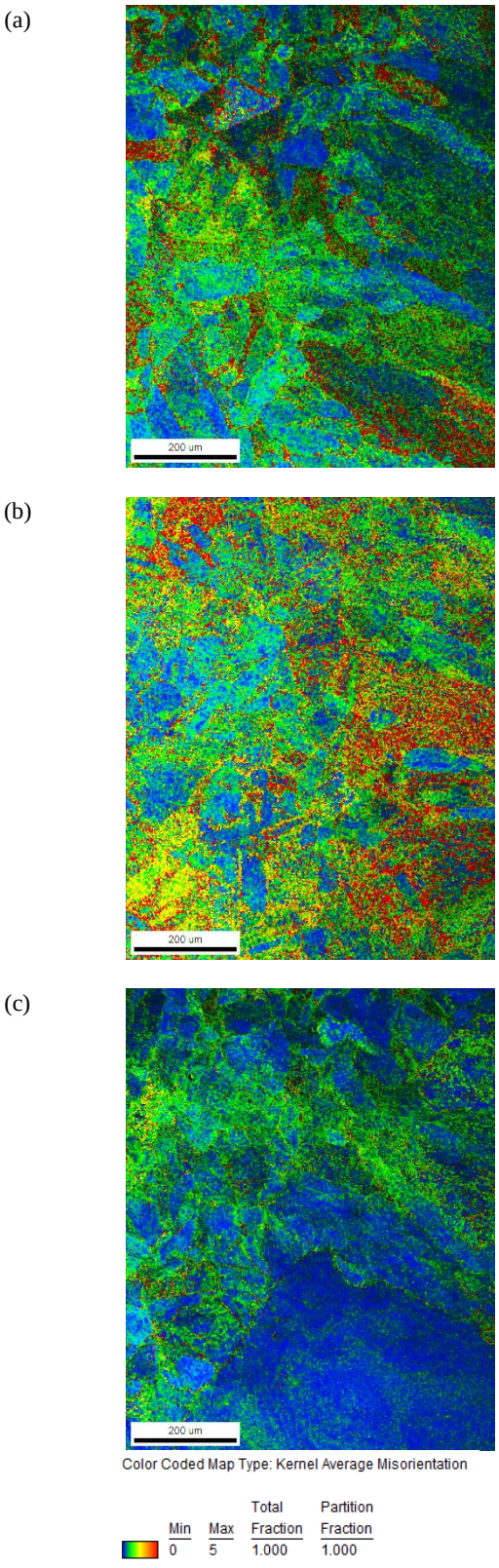

Figure. 4. KAM mapping on Alloy 600 HAZ distance from the fusion boundary about 700μm. Above three pictures show KAM distribution of (a) As-welded, (b) HT400_Y15, and (c) HT400_Y30 specimens.

	KAM	As-welded			HT400_Y15			HT400_Y30		
		Fraction (%)		KAM * %	Fraction (%)		KAM * %	Fraction (%)		KAM * %
low degrees	0.125	0.01934	0.76325	0.0024175	0.04742	0.6503	0.0059275	0.03412	0.88136	0.004265
	0.375	0.18707		0.07015125	0.18281		0.06855375	0.37161		0.13935375
	0.625	0.336		0.21	0.25385		0.15865625	0.327		0.204375
	0.875	0.22084		0.193235	0.16622		0.1454425	0.14863		0.13005125
high degrees	1.125	0.10764	0.20707	0.121095	0.09837	0.23861	0.11066625	0.06079	0.10767	0.06838875
	1.375	0.05386		0.0740575	0.06197		0.08520875	0.02673		0.03675375
	1.625	0.02885		0.04688125	0.04451		0.07232875	0.01301		0.02114125
	1.875	0.01672		0.03135	0.03376		0.0633	0.00714		0.0133875
very high degrees	2.125	0.00975	0.02969	0.02071875	0.02723	0.1111	0.05786375	0.00396	0.010966	0.008415
	2.375	0.00635		0.01508125	0.0217		0.0515375	0.00234		0.0055575
	2.625	0.00426		0.0111825	0.01636		0.042945	0.00142		0.0037275
	2.875	0.00287		0.00825125	0.01224		0.03519	0.000898		0.002580456
	3.125	0.00192		0.006	0.00886		0.0276875	0.000629		0.001965072
	3.375	0.00117		0.00394875	0.00635		0.02143125	0.000543		0.001832051
	3.625	0.000871		0.003156208	0.00447		0.01620375	0.000371		0.00134431
	3.875	0.000516		0.001999333	0.00279		0.01081125	0.000193		0.000749751
	4.125	0.000478		0.001973132	0.00204		0.008415	0.000188		0.00077595
	4.375	0.000365		0.001598931	0.00158		0.0069125	0.000156		0.000681896
	4.625	0.000199		0.000919718	0.00132		0.006105	0.00015		0.000696002
	4.875	0.000941		0.004585167	0.00616		0.03003	0.000118		0.00057642
total		1.00001	1.00001	**0.828594**	1.00001	1.00001	**1.025206**	0.999996	0.999996	**0.646621**

Figure. 5. Total averaged KAM value of each case. As-welded, HT400_Y15, and HT400_Y30 respectively.

The other preceding researches [11, 12] explained that post-weld heat treatment (PWHT) affects residual stress distribution on the material. When the heat applied to the material, residual stress relaxation occurs since heat can deform the material by decreasing yield strength of it [12]. So, it can be said that this phenomenon is happened similarly when the material undergoes the thermal aging process.

The KAM mapping of aged specimen by 15 years shows that residual strains are distributed broadly. It can be treated as residual stress distribution. And following the result of hardness test, it can be said that the type of residual stress is tensile.

The reason why hardness increases a little bit compared to As-welded except the point at 35 μm far from the fusion line is since the amount of stress decreases due to relaxation.

When the material thermally aged by 30 years, remained residual stress almost disappears so that the hardness increases generally.

4. Conclusions

This study was conducted to investigate how thermal aging affects residual stress and residual strain distribution of Alloy 600 HAZ. Following conclusions can be drawn from this study.

According to preceding researches and this study, both the relaxation of residual stress and the change of residual strain follow as similar way, spreading out from concentrated region.

The result of Vickers micro-hardness tester shows that tensile residual stresses are distributed broadly on the material aged by 15 years. Therefore, HT400_Y15 material is weakest state for PWSCC.

The value of residual strain measured by EBSD is largest when the material thermally aged by 15 years. This means HT400_Y15 material is weakest state for PWSCC.

In conclusion, the material thermally aged by 15 years is the most vulnerable to PWSCC.

ACKNOWLDEGEMENT

This work was financially supported by the International Collaborative Energy Technology R&D Program (No. 20168540000030) of the Korea Institute of Energy Technology Evaluation and Planning (KETEP) which is funded by the Ministry of Trade Industry and Energy.

REFERENCES

[1] J. Kai, G. Yu, C. Tsai, M. Liu, and S. Yao, The Effects of Heat Treatment on the Chromium Depletion, Precipitate Evolution, and Corrosion Resistance of Inconel Alloy 690, Metallurgical Transactions A, Vol.20, p.2057, 1989.
[2] S. Yamazaki, Z. Lu, Y. Ito, Y. Takeda, and T. Shoji, The Effect of Prior Deformation on Stress Corrosion Cracking Growth Rates of Alloy 600 Materials in a Simulated Pressurized Water Reactor Primary Water, Corrosion Science, Vol.50, p.835, 2008.
[3] Z. Lu, J. Chen, T. Shoji, Y. Takeda, and S. Yamazaki, Characterization of Microstructure, Local Deformation and Microchemistry in Alloy 690 Heat-Affected Zone and Stress Corrosion Cracking in High Temperature Water, Journal of Nuclear Materials, Vol.465, p.471, 2015.
[4] C. Miyasaka, B.R. Tittmann, and S.I. Tanaka, Characterization of Stress at a Ceramic/Metal Joined Interface by the V(Z) Technique of Scanning Acoustic Microscopy, Journal of Pressure Vessel Technology-Transactions of the Asme, Vol.124, p.336, 2002.
[5] D.R. Kwak, S. Yoshida, T. Sasaki, J.A. Todd, and I.K. Park, Evaluation of near-Surface Stress Distributions in Dissimilar Welded Joint by Scanning Acoustic Microscopy, Ultrasonics, Vol.67, p.9, 2016.
[6] L. Wang, H. Bei, Y.F. Gao, Z.P. Lu, and T.G. Nieh, Effect of Residual Stresses on the Hardness of Bulk Metallic Glasses, Acta Materialia, Vol.59, p.2858, 2011.
[7] 2010 ASME Boiler and Pressure Vessel Code, Section IX: Welding and Brazing Qualifications, Includes 2011 Addenda Reprint, ASME 2010.
[8] K.J. Choi, J.J. Kim, B.H. Lee, C.B. Bahn, and J.H. Kim, Effects of Thermal Aging on Microstructures of Low Alloy Steel–Ni Base Alloy Dissimilar Metal Weld Interfaces, Journal of Nuclear Materials, Vol.441, p.493, 2013.
[9] Z. Lu, T. Shoji, S. Yamazaki, and K. Ogawa, Characterization of Microstructure, Local Deformation and Microchemistry in Alloy 600 Heat-Affected Zone and Stress Corrosion Cracking in High Temperature Water, Corrosion Science, Vol.58, p.211, 2012.
[10] C. Ma, J. Mei, Q. Peng, P. Deng, E.-H. Han, and W. Ke, Microstructure Characterization of the Fusion Zone of an Alloy 600-82 Weld Joint, Journal of Materials Science & Technology, Vol.31, p.1011, 2015.
[11] H.-C. Jung, S.-W. Kim, Y.-H. Lee, S.-W. Baek, M.-S. Ha, and H.-J. Shim, Investigation of Effect of Post Weld Heat Treatment Conditions on Residual Stress for Iter Blanket Shield Blocks, Fusion Engineering and Design, 2016.
[12] P. Dong, S. Song, and J. Zhang, Analysis of Residual Stress Relief Mechanisms in Post-Weld Heat Treatment, International Journal of Pressure Vessels and Piping, Vol.122, p.6, 2014.